Journal of Engineering Physics and Thermophysics, Vol. 75, No. 5, 2002

REVIEW

APPLICATION OF MHD EFFECTS IN ELECTROLYTES FOR MODELING VORTEX PROCESSES IN NATURAL PHENOMENA AND IN SOLVING ENGINEERING-PHYSICAL PROBLEMS

N. F. Bondarenko, E. Z. Gak, and M. Z. Gak

UDC 536.2:538.4:583.692

This paper gives an overview of the experimental results obtained by the method of MHD modeling in thin electrolyte layers and used to solve problems connected with the appearance of monotonic and vibrational instabilities. Primary consideration is given to the generation and interaction of transient vortex processes. As examples, the results of the investigations of flows in systems of two, three, and four vortices and periodic vortex structures, as well as of flows in the presence of obstacles of different permittivity modeling plants or technogenic screening devices intended to protect objects against pollution are presented. We consider the ways of using the results obtained in studying natural phenomena and in solving engineering-technical problems connected with mass and heat transfer and electrotransmission.

Introduction. Fluid and gas flows, in which under the action of various factors the horizontal component of the velocity field is much larger than the vertical component, play an important role in both natural phenomena (atmospheric processes, ocean flows) and numerous technological processes. Moreover, in the last few years such flows in thin fluid layers have been extensively investigated under laboratory conditions [1–3].

The complexity of theoretical studies of nonlinear phenomena in shear flows, especially of the hydrodynamic instability in such systems, stimulated a search for novel methods which would make it possible to analyze such processes in a time good for visualization with the possibility of controlling the evolution of vortex structures. Of the laboratory methods of generation of vortex flows, such as the source-sink method, rotating vessel bottom, etc. [4–6], the method of flow generation under the action of magnetohydrodynamic forces proposed by the Agrophysical Institute in 1967 exactly for the purposes of modeling has apparently proved to be best suited for investigating the dynamics and kinetics of vortex structures in thin fluid layers [7, 8]. It received further development in joint investigations of the Agrophysical Scientific-Research Institute and the Institute of Atmosphere Physics of the Russian Academy of Sciences supported by Academician A. M. Obukhov [1–3, 5, 9–17]. It is available and visual, and its realization does not entail considerable costs and provides the possibility of getting to the bottom of many natural phenomena and engineering-technical problems associated with mass and heat transfer and electrotransmission [11–13].

In the present paper, primary consideration is given to the methods of generation, transformation, and visualization of vortex structures in thin electrolyte layers developed by the authors and their practical application. As examples, the results of investigations of the generation and interaction in systems of two-, three-, and four-vortex structures, as well as of the study of multivortex periodic structures (Kolmogorov flow), are presented. Materials on the generation of vortices in a stream at a flow around structures of different permittivity modeling plant or technogenic obstacles playing the role of devices screening from pollution the air and water in agricultural, water-development works, and in other engineering structures are presented.

Quasi-Two-Dimensional Shear Flows (Theoretical Premises). The possibility of generating by the MHD method controlled vortex flows has served not only as one of the prerequisites for developing theoretical fundamentals

Agrophysical Scientific-Research Institute, Russian Academy of Agricultural Sciences, St. Petersburg; email: ivl@agrophys.spb.su. Translated from Inzhenerno-Fizicheskii Zhurnal, Vol. 75, No. 5, pp. 186–196, September–October, 2002. Original article submitted September 7, 2001; revision submitted April 2, 2002.

 1062-0125/02/7505-1234$27.00

of hydrodynamic phenomena arising in thin fluid layers, but also as a stimulus to perform a large number of experiments in this field. The investigations have shown that correct theoretical description of processes where the vertical velocity component V_z is much smaller than the horizontal ones (i.e., $V_z << V_x$, $V_x << V_y$) is possible with consideration for not only the internal, but also the external friction against the bottom (and/or the cover). Here the external (near-bottom) friction plays the determining role in the development of vortex flows under various conditions (subcritical, critical, and supercritical), in the appearance and interaction of coherent structures and vibrations, and in the appearance of turbulence. What is more, only in this case is agreement between theoretical and experimental data observed (Kolmogorov flow, vibrations in the system of four vortices). For instance, F. V. Dolzhanskii [1–3] has shown that in this case the corresponding equations of two-dimensional hydrodynamics take on the form

$$\begin{gathered}\partial V_x/\partial t + V_x\,\partial V_x/\partial x + V_y\,\partial V_x/\partial y = -\rho^{-1}\,\partial p/\partial x + \nu\Delta V_x - \lambda V_x + F_x\,,\\ \partial V_y/\partial t + V_y\,\partial V_y/\partial x + V_y\,\partial V_y/\partial y = -\rho^{-1}\,\partial p/\partial y + \nu\Delta V_y - \lambda V_y + F_y\,,\\ \partial V_x/\partial x + \partial V_y/\partial y = 0\,.\end{gathered} \tag{1}$$

$$\lambda = 2k\nu/h^2\,, \tag{2}$$

where k is found experimentally and the possible inhomogeneity of F_x and F_y along z is taken into account. As noted in [3], the situation in the quasi-two-dimensional layer of fluid is controlled by two parameters, namely, by the traditional Reynolds number

$$\mathrm{Re} = UD/\nu\,, \tag{3}$$

and by the Reynolds number in view of (2)

$$\mathrm{Re}_\lambda = U/\lambda D\,. \tag{4}$$

In [2, 3], it is shown that at $\mathrm{Re}_\lambda << \mathrm{Re}$ the contribution of the internal viscosity is insignificant, at least under the conditions of a stable flow, and can be ignored in the calculations. For the case of vortex structures, system (1), according to [16], can be given in cylindrical coordinates as

$$\partial\xi/\partial t + [\xi, \Psi] = -\lambda\xi + \nu\Delta\xi + F\,. \tag{5}$$

Features of the MHD Modeling Method. As mentioned above, MHD modeling occupies a special place among the other methods of generation of vortex motion in a fluid [4–6] because it directly relates hydrodynamic, electrical, and magnetic phenomena and provides the possibility of isothermal excitation of a conducting fluid. The employment of the MHD-method makes it possible to obtain, at values of the current density up to j = 0.1 A/m^2 and magnetic induction B up to (0.1–0.3) T, that can easily be attained under laboratory conditions, fluid flows with velocities up to V = 1 m/sec, i.e., reach Reynolds numbers Re > 10^4, which creates prerequisites for using this method in studying the hydrodynamic instability, the formation of secondary flows, and the excitation of nonlinear capillary-gravity waves [18–20], including solitons [21]. Magnetohydrodynamic mass forces of density

$$\mathbf{F}_{\mathrm{MHD}} = [\mathbf{j}, \mathbf{B}] \tag{6}$$

arise in the bulk of the electrolyte under the action of crossed electric and magnetic fields of a certain configuration. In this case, in (1) and (5) $\mathbf{F} = \rho^{-1}\mathbf{F}_{\mathrm{MHD}}$.

A convenient characteristic of the flow instability is the evaluation of the flow conditions by the supercriticality value s, according to [3], where

$$s = j/j_{\mathrm{cr}} - 1\,. \tag{7}$$

As a critical value of the electric current density the flow loses stability. Since the value of j determines the flow velocity V and, consequently, the Re and Re_λ numbers, in a number of cases, to estimate the character of the flow, one also uses

$$s = \mathrm{Re}_\lambda / \mathrm{Re}_{\lambda,\mathrm{cr}} - 1 . \tag{8}$$

Let us dwell on the general features of the experimental procedure. Use of $\mathbf{F}_{\mathrm{MHD}} \neq 0$ makes it possible to set in motion the horizontal thin fluid layer filling a flat cell if electric current is conveyed to it conductively and an inhomogeneous magnetic field is created in it due to the open magnetic systems located under the cell bottom. As sources of such a field, magnetic systems formed on the basis of standard permanent magnets can be used. An inhomogeneous magnetic field can be formed, for example, on the surface of a sheet ferroelast [22, 23], which permits obtaining surfaces of models of unlimited extent (up to 1 m^2 and more). A thin fluid layer of height $h = (5–10)\cdot 10^{-3}$ m permits creating a small value of grad B_z, practically grad $B_z \to 0$, and, consequently, the $\mathbf{F}_{\mathrm{MHD}}$ value in (6) will be largely determined by the fluid surface coordinates (x and y) and can be constant with height, i.e., $\mathbf{F}_{\mathrm{MHD}} \neq f(z)$. In this case, the relation between the pole sizes and the electrolyte layer thickness is selected from the condition of a small change in B_z at $0 \leq z \leq h$. Moreover, MHD effects can be attained in complete absence of flow fluctuations, which is difficult to obtain by other familiar methods.

To generate vortex flows in thin electrolyte layers, flat closed rectangular or round cells with copper electrodes located on the side walls were used. One can realize the required distribution of MHD forces in the flow plane, where

$$\mathrm{rot}\, \mathbf{F}_{\mathrm{MHD}} = \mathrm{rot}\, [\mathbf{j}, \mathbf{B}] = (\mathbf{B}\, \mathrm{grad})\, \mathbf{j} - (\mathbf{j}\, \mathrm{grad})\, \mathbf{B} \neq 0 . \tag{9}$$

In our case, it is convenient to use the following conditions: grad $B \neq 0$, grad $j = 0$, and $j \neq 0$. The current is usually time-invariant. Moreover, such a method makes it possible to form flows with an "inflection point" or an "inflection zone" [5] in the velocity profile, which is difficult to do by other methods.

We used the following system: copper electrodes–(1.0–1.5) N solution of $CuSO_4$ [7–10], the current values thereby were selected in the region of electrochemical kinetics, in a zone far from gas release, and in the range of limiting current densities [7, 8]. The presence of a free surface and the relatively long-time interaction of the vortex structures ($\tau \approx 60$ sec) permits observing stationary and nonstationary motions of the electrolyte both visually and by the methods of photographing, filming, and video filming.

As tracer particles, we used leucopodium seeds and aluminum powder. By the particle tracks and the time of filming or photographing a frame local velocities or velocity fields on the fluid surface were determined. The present-day methods of image processing with the use of video and computer facilities make it possible not only to obtain qualitative results, but also give information in the form of a velocity field under different experimental conditions [3, 14, 15] and determine, by the data found with the aid of a video camera, the pressures in the fluid and λ values from (2).

Thus, because of the small value of h, the friction against the bottom raised the stability threshold of the free surface, which enabled us to observe the development and formation of secondary stationary and fluid-induced vibrational flows in the range of velocities $V = (0.01–0.1)$ m/sec.

Evolution of Vortex Structures. For laboratory modeling of the transient condition of flows, of particular interest are methods of generation of individual elementary vortex structures (a single vortex, vortex pairs) using which one can model a vortex structure of a real flow as a whole. This section presents the results of investigations of the formation of elementary "mushroom-like" or, according to [24], "bipolar" structures. In this case, $\mathbf{F}_{\mathrm{MHD}}$ = const. During the experiment, the evolution of vortex structures and their transformation from small-scale single vortex structures into an integral structure of a larger scale were investigated. In [25], we consider two original cases of the generation by the MHD method of vortex structures in the form of two or three vortices excited in a thin layer of an electrolyte placed in rectangular and triangular cells and the phenomena of monotonic instability of these vortices. To investigate the process of the formation and visualization of two-dimensional "mushroom-like" structures, we used the facility illustrated in Fig. 1a. It incorporates a flat rectangular cell 1 of area $a \times b$ (a = 0.3 m, b = 0.2 m) and height m = 0.015 m with a bottom thickness d_0 = 0.002 m. The cell is filled with a water electrolyte (1.5 N $CuSO_4$) 2 to a depth

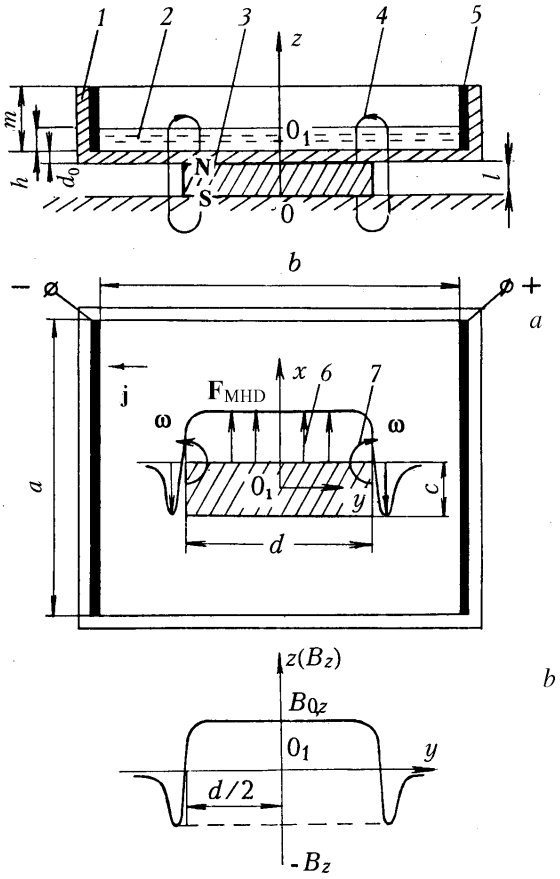

Fig. 1. Generator of the "mushroom-like structure": a, [1) rectangular cell; 2) electrolyte layer of thickness $h = 5 \cdot 10^{-3}$ m; 3) flat rectangular magnet; 4) lines of force of a constant magnetic field with induction B; 5) flat copper electrodes; 6) profile of magnetodynamic forces $\mathbf{F}_{MHD}$ arising in the flow planes; 7) vortices with angular rotational velocity ω; 0 and 0_1, center of xy coordinates and projection of the center 0 on the cell bottom, respectively]; b, distribution of magnetic field induction B_z along the y-axis.

h = 0.005 m. Under the cell bottom, a permanent rectangular magnet 3 of height l = 0.15 m with sides of d = 0.08 m and c = 0.02 m was located. The vertical magnetic field B_z 4 is sign-changing in space, which is due to the homogeneous field with induction $B_{0,z}$ = 0.08 T on the magnet surface at y = 0 and the scattering fields (edge effects). The diagram of the B_z distribution along the y-axis is given in Fig. 1b. The copper electrodes 5 are fixed on the cell walls. Direct electric current I = 0.35 A invariable during the experiment was fed into the cell filled with a fluid. The current density vector is directed along the y-axis. Figure 1a shows a diagram of the magnetohydrodynamic force acting along this axis. The process kinetics was registered at certain time intervals as soon as electric current was turned on, as is seen from Fig. 2.

Figure 3a gives the scheme of the generation of two vortices of equal intensity. The cell 1 0.09 × 0.16 m in size is filled with electrolyte 2 to a depth h = 0.005 m. Under the cell, a magnetic system 3 of four magnets is located. Each pair of magnets consists of rectangular ferrite plates magnetized in the axial direction. The distribution of the vertical component B_z is given in Fig. 3b. Figure 3a shows the dependences $\mathbf{F}_{MHD}(y)$ and the directions of motion of the generated vortices. Figure 4 shows the photographs of the observed structures. The facility for the generation of three vortices is made in the form of a cell shaped as an equilateral triangle with 0.16 m sides (Fig. 5). Two pairs of magnets each were placed in the vertices of the triangle so that the neutral line of the magnetic system was directed along the bisectrix of the triangle angles at a distance of 0.05 m from the vertex. The electrodes were located at a distance of 0.03 m from it.

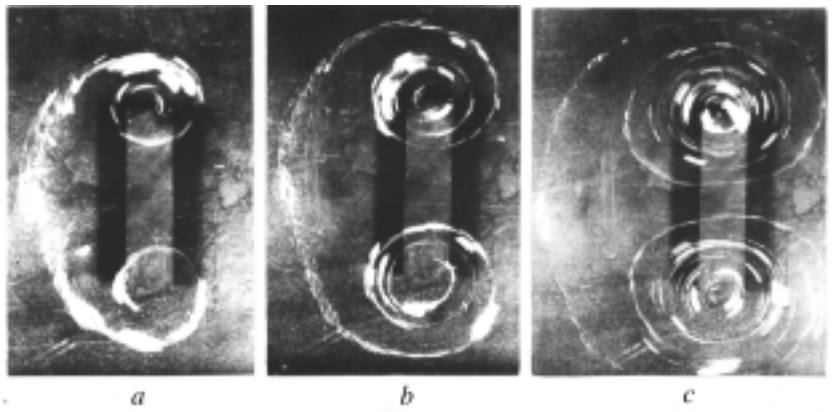

Fig. 2. Photographs of the formation and evolution of "mushroom-like structures" arising in the fluid layer under the action of a two-dimensional shear jet flow. Exposure of 4 sec. The photographs were taken after electric current I = 0.25 A was turned on: a) after t = 30, b) 45, and c) 60 sec.

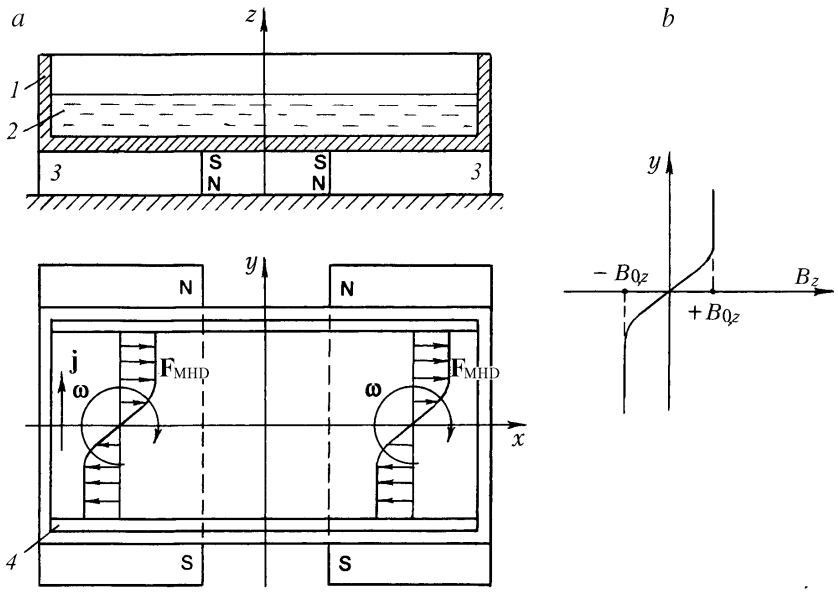

Fig. 3. Scheme of the generation of two vortices of equal intensity: a, [1) rectangular cell; 2) electrolyte; 3) magnetic system consisting of two rectangular magnets; 4) electrodes)]; b, B_z distribution along the y-axis at the center of the magnetic systems.

Consider the results obtained. As is seen from Fig. 2a, as soon as current was turned on, there appeared a fluid jet of width d and two reverse flows under the action of the magnetic scattering field at the magnet edges. The arising couples of forces create at the magnet edges vortices 7 (see Fig. 1) rotating in opposite directions with frequency ω. In the time τ = 60 sec (Fig. 2a), the "mushroom-like structure" has considerably grown in size. The symmetry axis of the structure is perpendicular to the current direction. The growth of the vortex dimensions is limited to the cell dimensions a and b. The velocity of motion of the leading portion of the structure is of the order of V_f = $(2–3)\cdot10^{-3}$ m/sec.

The experimental procedure schematically represented in Fig. 3 makes it possible to create in the bulk of the flat layer two couples of forces under the action of which two vortices with dimensions of the order of the cell width arise, and the intensity, the size, and the directions of rotation with angular velocity ω were determined by the values of $\mathbf{j}$ and $\mathbf{B}_z$. As follows from the experiments, when the vortices rotate in opposite directions, the pattern of the vortex structures is stable. Under natural conditions the vortices should move apart; however, in the experiment their dimen-

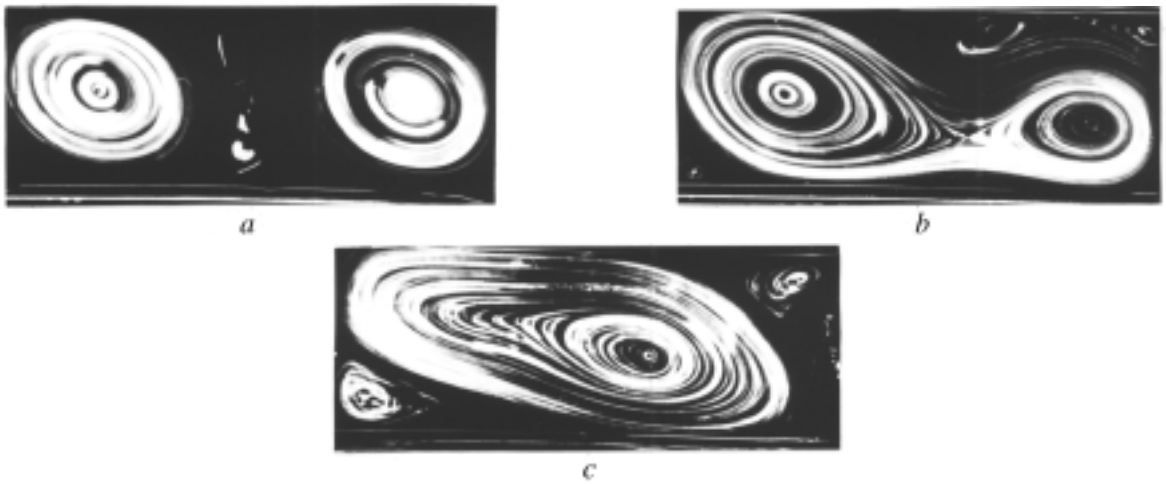

Fig. 4. Patterns of the generation of two vortices of equal intensity and directions: a) $j < 1 \cdot 10^2$ A/m^2; b) $1 \cdot 10^2$ A/m^2 $< j < 2 \cdot 10^2$ A/m^2; c) $j = 2 \cdot 10^2$ A/m^2.

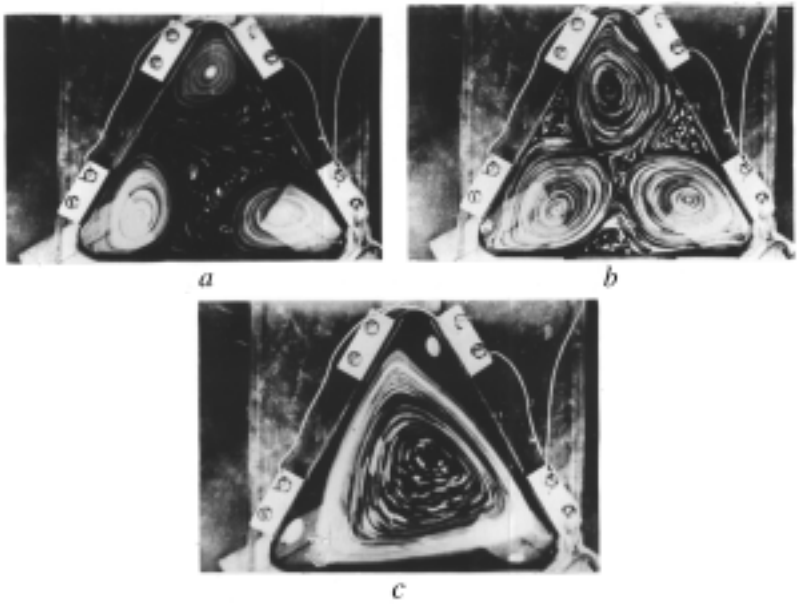

Fig. 5. Patterns of the generation of three vortices of equal intensity and directions: a) $j < 1.5 \cdot 10^2$ A/m^2; b) $1.5 \cdot 10^2$ A/m^2 $< j < 3 \cdot 10^2$ A/m^2; c) $j = 3 \cdot 10^2$ A/m^2.

sions are limited to the cell width. Figure 4 gives an example of the same direction of rotation of vortices. Figure 4a shows the appearance of two vortices. With increasing current density, instability of the flow is noted (Fig. 4b), the dimensions of the vortices increase, there appears a bridge between them, and then, at $j = j_{cr}$ they merge ($j_{cr} = 1.5 \cdot 10^2$ A/m^2). A single vortex with a scale of the cell length arises (Fig. 4c). Note that an analogous situation also takes place in the case of the generation of three vortices (Fig. 5). In the vertices of the triangular cell, first three vortices are observed (Fig. 5a), then they grow with increasing j (Fig. 5b) and merge into a single vortex structure with a scale corresponding to the cell dimensions (Fig. 5c). In so doing, in the cell vertices vortices of a smaller scale are initiated.

Two-dimensional "mushroom-like structures" occur naturally. They arise, for example, when a jet enters a still fluid. Therefore, the process of the formation of such structures and their interaction with one another and with other stationary objects is of interest. Thus, one can observe analogies between our photographs (Figs. 2, 4) with other flow patterns [11, 12] and the photographs of dust storms, synoptical vortices, cyclonic perturbations, and a typhoon presented, in particular, in [26, 27]. Under natural conditions, the role of tracers-visualizers is played by particles of ice,

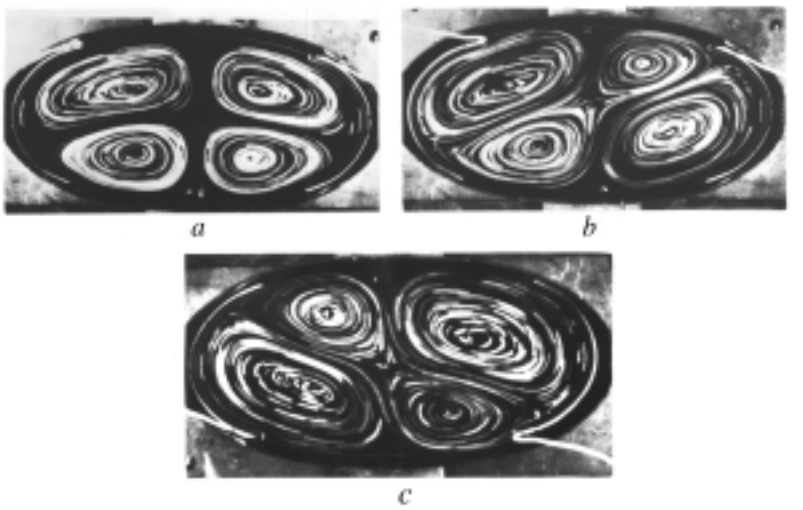

Fig. 6. Visualization of flows at fluid-induced vibrations of vortex flows: a) four-vortex flow in the oval cell under subcritical conditions at I = 0.2 A and exposure of 4 sec; b, c) fluid flows under fluid-induced vibrations for two limiting phases at I = 0.3 A and exposure of 2 sec.

vapor, and dust. Apparently, MHD modeling can be useful for gaining insight into the evolution of similar structures in nature with time or under the action of various physical factors.

We now dwell on the phenomenon of emergence of vortex structures (Figs. 4, 5). In modern theories of turbulence, it is customary to assume that normal energy transfer from the central macrovortex flows to the periphery with their splitting into small vortices is followed by energy dissipation because of the wall friction and its transformation to heat [5]. However, this effect, often called the "Kolmogorov cascade," arises at very high Reynolds numbers [28]. In the case of two-dimensional turbulence, the Reynolds numbers are much lower than the critical ones. Obviously, the "negative viscosity" effect or the phenomenon described by it [29–32] (when not normal energy transfer from the center of the flow to its boundaries, but, vice versa, from the periphery to the center occurs) can be one of the basic sources of instability of the flow in the primary mechanism of the appearance of turbulence. For instance, in a number of experimental works, it has been shown that exactly in the boundary layers of the flow (water media, dielectric fluids) at fluid motion there occurs continuous transfer to the center of hydrodynamic structures (microvortices, vortex cores, gas bubbles), which are initiated at the periphery due to the appearance of the vertical velocity component and are likely to carry noncompensated electric charges [33–37]. A number of similar phenomena are also observed in the atmosphere when heated air jets are going up from the earth [29].

A further theoretical description of the results obtained here can be carried out in solving Eq. (5), taking into account the form of the dependence of $\mathbf{F}_{\mathrm{MHD}}$ by (6) with the use of the graphically given dependence $\mathbf{F}_{\mathrm{MHD}} = f(y)$ (Figs. 1, 3).

Generation and Investigation of Fluid-Induced Vibrations. With increasing pressure in a two-dimensional fluid layer at values of $s > 1$, it turned out to be possible to observe the appearance of fluid-induced vibrations in the system of vortex structures, their periodic reconnection, and a number of other unusual effects. As an example, the results of the generation of fluid-induced vibrations in the system of four vortices and under interaction of electrolyte counter jets are given.

System of four vortices. An experimental study of these effects was first made in [38] and then in [39], and their theoretical analysis was performed in [40]. Stable fluid-induced vibrations in the system of four vortices, whose period depended on the external excitation intensity and the fluid depth, were observed visually. For laboratory investigations, a flat horizontally arranged oval cell 0.115 × 0.23 m in size with a bottom thickness of 0.002 m filled with 1 N $CuSO_4$ was used. The diagram of the plant and the distributions of B_z and j are given in [38]. Figure 6 shows the photographs of the vortex structures in excited fluid-induced vibrational processes. It should be noted that such flows also arose in the Hele–Shaw cell at thermoconvection [41]. However, upon MHD excitation [40], a pure isothermal mode of fluid-induced excitation of vibrations takes place (they appeared due to the internal mechanisms of insta-

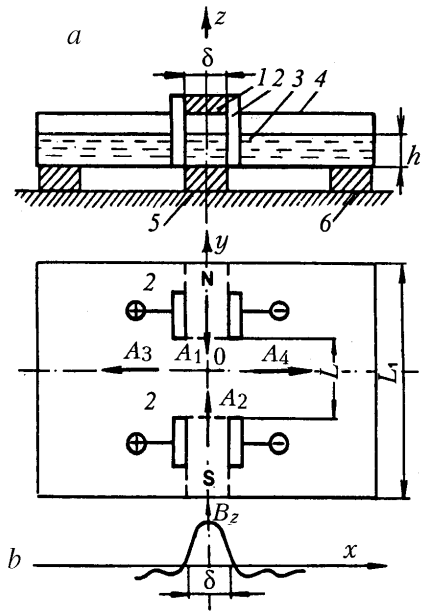

Fig. 7. Schematical representation of the plant for investigating the interaction of counter jet flows upon their head-on collision: a, [1) insulating liner whose width δ corresponds to the jet width; 2) copper electrodes; 3) electrolyte; 4) cell; 5) flat rectangular magnets; 6) support for mounting the cell]; b, B_z distribution along the *x*-axis.

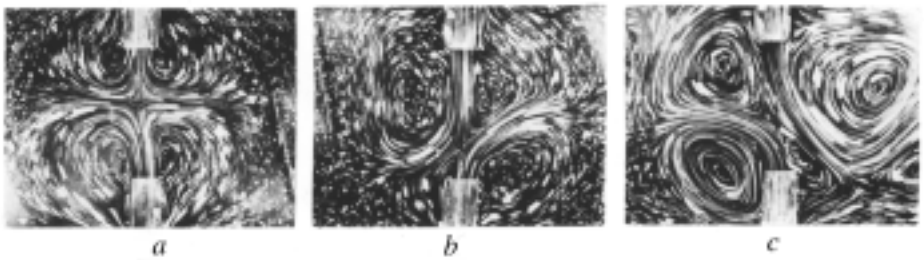

Fig. 8. Photographs of flows arising at a head-on collision of two counter jets: a) subcritical conditions of vibrations ($Re_\lambda/Re_{\lambda,cr} < 1$); b and c) flows arising under fluid-induced vibrations at $Re_\lambda/Re_{\lambda,cr} \approx 2$ at a periodic deviation of the jets from the symmetry axis for two limiting vibration phases and exposure of 2 sec.

bility without the action of time-variable external forces). In all events, constant energy was fed into the system, since j = const and B_z = const.

Electrolyte counter jets. Laboratory studies of the jet flows were carried on a plant (Fig. 7) incorporating a flat horizontally arranged 0.3 × 0.2 m cell with a transparent bottom. The cell was filled with an electrolyte (1 N $CuSO_4$), whose depth was varied over the range of 0.003–0.015 m, and positioned on a magnetic system of two ferrite rectangular magnets 0.025 × 0.12 m in size. To create a jet outflowing from the channel (nozzle), we used two pairs of copper electrodes located over the side edges of the magnet and separated by an insulating liner. The electrodes were located at a distance of 1 cm from the side walls. With a proper choice of the current direction, jets A_1 and A_2 directed towards each other arise; they collide with each other and separate at a right angle in the form of jets A_3 and A_4. In Fig. 8, one can see the stationary pattern of vortex structures. The arrangement of the plant makes it possible to smoothly change the fluid velocity from zero to 0.1 m/sec. At $s > 1$ the stationary flow loses stability and a fluid-induced vibrational motion of the fluid arises. It is characterized by the fact that the jets periodically deviate from the symmetry axis in opposite directions and are separated by two vortices, which can be thought of as analogs of the vortex layer (Fig. 8b and c).

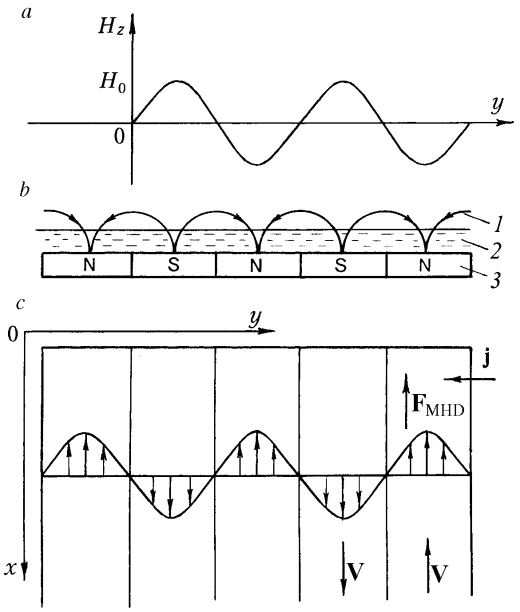

Fig. 9. Distribution of the magnetic field strength and forces in the experimental plant for generating two-dimensional periodic flows: a) profile of the vertical component of the magnetic field strength H_z (A/m); b) profile of the tangential component of the magnetic field strength **H** (A/m) [1) magnetic field lines; 2) electrolyte layer; 3) magnetoelastic rubber)]; c) profile of the force $\mathbf{F}_{MHD}$ acting on the electrolyte during the passage of direct current of density **j**.

Fluid-induced vibrations excited in the closed horizontal fluid layer can model global atmospheric processes. The results obtained permit solving other applied problems as well. For example, the organization of the mixing of warm air in greenhouses or phytochambers for their heating and a uniform distribution of carbon dioxide and other atmospheric gases in closed volumes can be considered. As the experimental results show, one should expect a more effective mixing of warm air in ellipsoidal systems than in rectangular ones where stagnant zones arise.

Modeling of Two-Dimensional Periodic Flows. The laboratory modeling of the Kolmogorov flow [1, 5] considered below has served as a powerful stimulus to develop a similar method of modeling in geophysical hydrodynamics. Along with the experimental study of this problem, it has also been studied theoretically. Equations (1) for fluid motion in a thin layer under the action of a periodic driving force proposed by F. V. Dolzhanskii [5] have been solved under the condition that

$$\mathbf{F}_{MHD} = jB \sin p_1 y \,. \tag{10}$$

The above-mentioned flow was only proposed as a convenient object for theoretical investigations. Such flows received the name "vortex parquet" [5]. The laboratory model was a rectangular 0.3 × 0.2 × 0.2 m cell with a transparent 0.002-m-thick bottom filled with a water solution (1 N $CuSO_4$) to a depth h = 0.03–0.05 m. Direct electric current was passed through the electrolyte in the transverse direction. The cell was placed on a 0.24 × 0.12 × 0.002 m magnetoelastic rubber sheet, which served as a magnetic field source. On the surface of the sheet, by special magnetization a system of poles in the form of 0.022-m-wide and 0.24-m-long bands with an alternating polarity was formed (Fig. 9). The neutral lines between the poles were parallel to the x-axis, i.e., perpendicular to the current direction. Such a system created a magnetic field strength with a profile close to a sinusoidal one. The plant parameters permitted variation of the j value from zero to $1.3 \cdot 10^2$ A/m^2. It has been found that at $j < 3 \cdot 10^2$ A/m^2 the fluid flow has a profile analogous to the profile of the external force, and at $j > 3 \cdot 10^2$ A/m^2 it becomes unstable, as a result of which a stationary flow consisting of a chain of vortices is formed. The flow patterns for various j are given in Fig. 10. They are considered in more detail in [1–3, 5, 11–13]. The results obtained have been described theoretically and repeatedly discussed and verified [42–47].

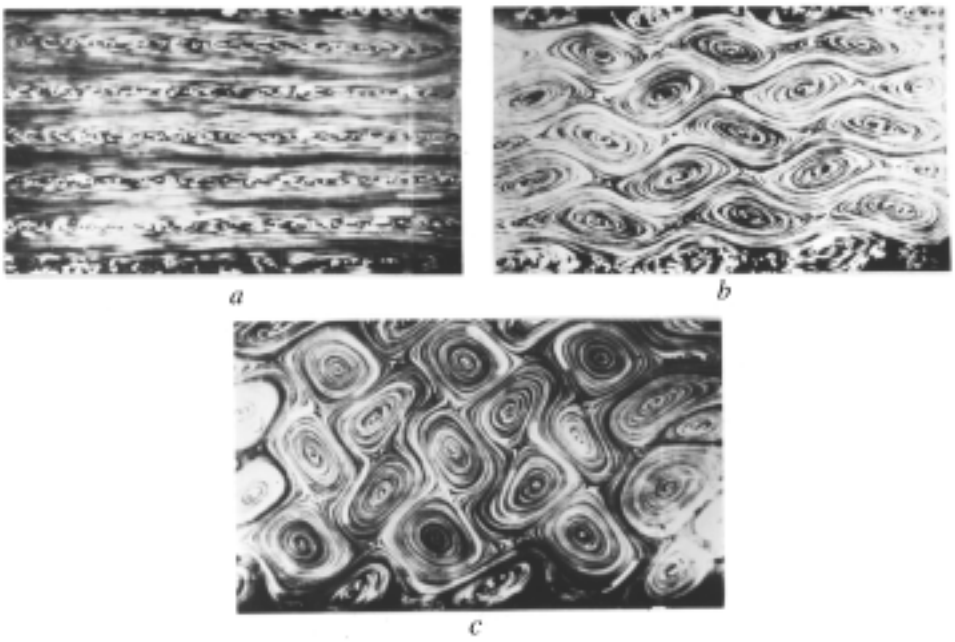

Fig. 10. Evolution of the pattern of the (A. N. Kolmogorov) plane-periodic flow with increasing current density ($H_0 = 1.6 \cdot 10^4$ A/m, layer depth $h = 3 \cdot 10^{-3}$ m): a) subcritical laminar condition with a sinusoidal profile of velocity ($j = 2 \cdot 10^2$ A/m^2, $\mathrm{Re}_\lambda/\mathrm{Re}_{\lambda,cr} < 1$); b) supercritical conditions, structure of the secondary flow at $j = 5.3 \cdot 10^2$ A/m^2, $\mathrm{Re}_\lambda/\mathrm{Re}_{\lambda,cr} = 2.5$; c) structure of the secondary flow at a higher level of supercriticality $j = 6.4 \cdot 10^2$ A/m^2, $\mathrm{Re}_\lambda/\mathrm{Re}_{\lambda,cr} = 4$.

Vortex Formation in Permeable Structures. Modeling of the interaction of a turbulent plane-parallel fluid or gas flow with a permeable asperity is of interest for investigating engineering constructions and the interaction of wind with a vegetation layer. Such problems are also interesting in solving problems associated with the investigation of the fluid motion through regular grates in stagnant reservoirs, in developing a method for improving the regime of natural water purification [48, 49], and for preventing domestic and farming buildings from being polluted with natural and anthropogenic substances and gases [50–52].

Since plant communities of various spatial-geometric structures represent for an air flow a permeable asperity, in the interleaf space there appear large-scale secondary structures of flows (vortices) largely determining the energy and mass transfer in plants. The flow characteristics depend on both the parameters of the wind flow over the plants and inside of them and the spatial-geometric characteristics of the plant community itself, the thickness and height of plants, and their air resistance [50].

For the laboratory modeling of such an interaction in the quasi-two-dimensional approximation, special methods were elaborated. In our case, the MHD effects were only used to generate a flow with a smoothly regulated velocity in a thin layer beyond the region of interaction between the flow and an obstacle modeling a plant cover [13, 53–57]. In our experiments, in a flat channel two compartments were formed: a narrow compartment for the MHD flow generation and a wide one, into which elements modeling an asperity were introduced. In the course of laboratory investigations, two types of arrangement of obstacles were used: (1) obstacle elements were located near the channel wall perpendicular to it and the incident flow velocity vector $\mathbf{V}_{in}$ (Fig. 11) and (2) obstacles in the form of permeable structures were positioned in the channel center also perpendicular to the flow velocity (Fig. 12). In the course of experiments, we varied the values of the flow velocities, the structure and geometry of the asperity elements, and the degree of "crowdedness" of permeable structures made from polyethylene needles.

The obstacle-flow interaction is illustrated in the photographs (Fig. 11): a, the flow is absent; b, the flows at the boundary with the spatial structure model (V_S) are insignificant and the "plants" are not air-blown; c, intense vortex formation is observed, and the vortex dimensions thereby are determined by the structure elements, which corresponds to complete air-blowing and intensive gas exchange. Figure 12 gives another example of permeable plants correspond-

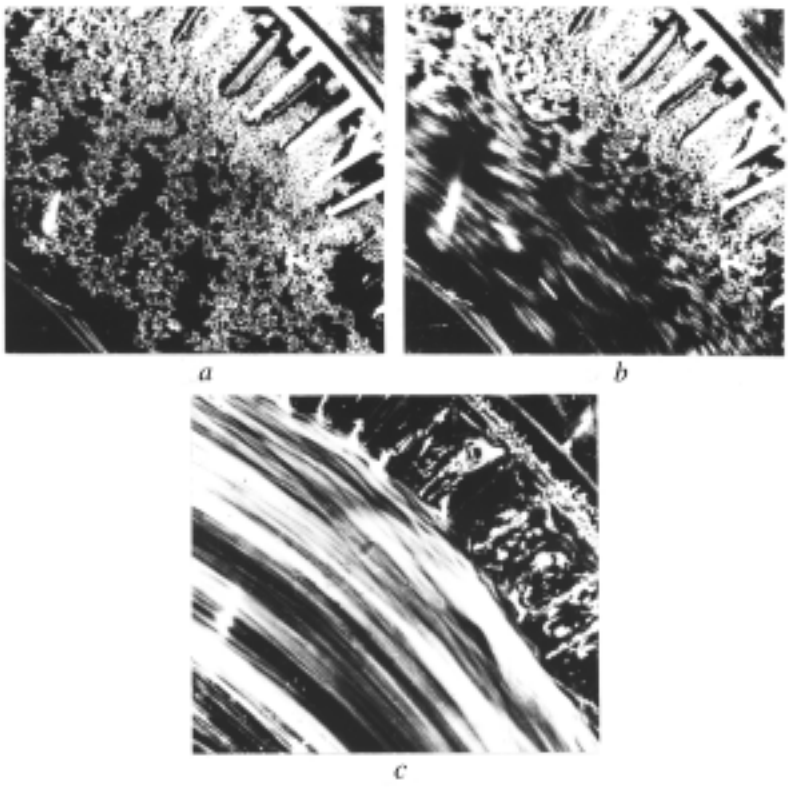

Fig. 11. Models of the interaction of wind with permeable structures (plants): a) I = 0, V_p = 0; b) I = 0.2 A, V_p = 0.001 m/sec; c) I = 6 A, V_p = 0.08 m/sec.

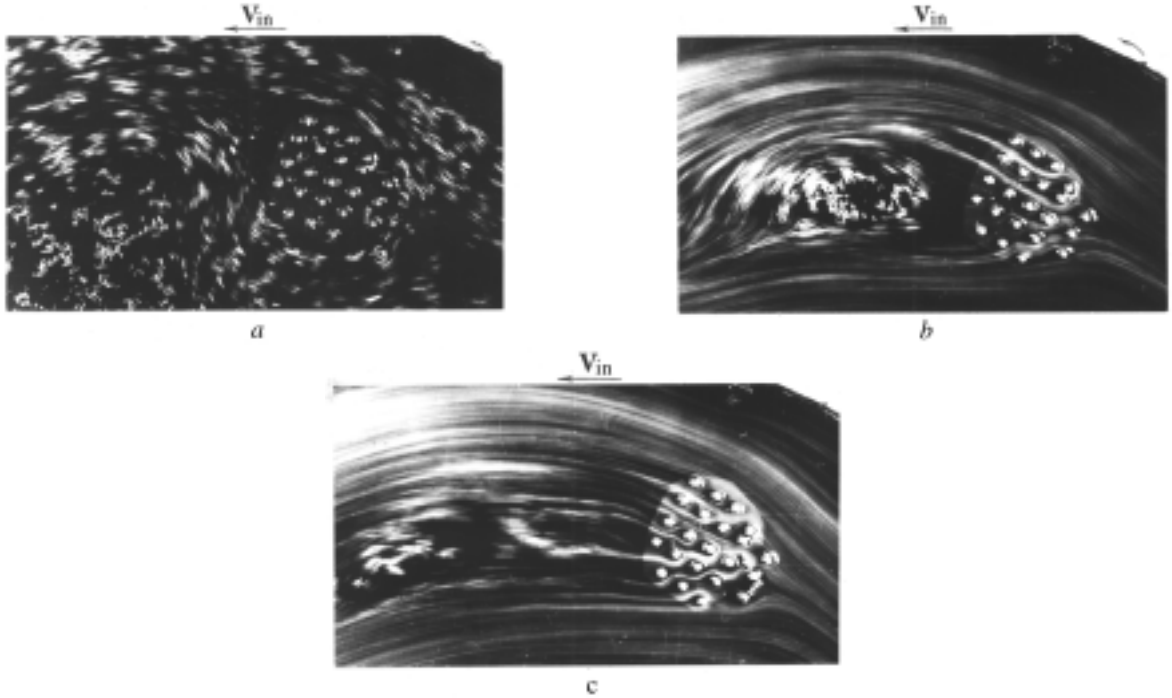

Fig. 12. Interaction of the two-dimensional flow with permeable cylindrical structures (diameter of the obstacle base — 0.3 m): a) I = 0.05 A, V_{in} = 0.001 m/sec; b) 0.1 and 0.01; c) 0.4 and 0.025.

ing to the theoretical problem on the role of a "hill with plants" intended to screen buildings from heavy particles [51]. From the results obtained it is seen that at small "creeping" velocities the obstacle is flown as a solid body similarly to the classical case and the screening effect is absent (Fig. 12a). With increasing velocity of the flow the fluid jets penetrate into the obstacle and its blowing begins (Fig. 12b). The single vortex formed behind the obstacle "slides" down the stream (Fig. 12c) until it completely scatters. In so doing, the classical case of the formation of two intermittent vortices — the Karman trail — is not observed and the structure is completely permeable. Behind the permeable obstacle there is no vertical component of the flow velocity and the vortex formation and soil erosion are absent. Such a system is effective for screening. However, conventional mathematical calculations for the case of heavy particles are very complicated and awkward. Therefore, the obtained qualitative and quantitative experimental results on the registration of the processes of mass transfer at different velocities of the carrier medium (electrolyte solution) and variations of the properties of a permeable asperity can be used in selecting proper criteria for verifying mathematical models and evaluation calculations.

CONCLUSIONS

The magnetohydrodynamic method makes it possible to smoothly change the Reynolds numbers in a thin electrolyte layer and observe different kinds of stationary and periodic motions, for example, the generation of fluid-induced vibrations and the processes of mergence and generation of vortex structures. It is useful in constructing mathematical models of complex geophysical systems as well as of various engineering structures, since the problem of investigating the hydrodynamic instability and the mechanisms of nonlinear interaction of vortex perturbations is of fundamental importance for the whole of hydrodynamics [58].

From the experimental results presented it follows that this method makes it possible to study simple but basic types of motions on which, as noted in [59–61], it is possible to effectively verify the fundamental theoretical notions and develop new principles awaiting to be given mathematical form.

NOTATION

V, flow velocity, m/sec; ω, angular rotational velocity of vortices in the cell, rad/sec; t, time, sec; ρ, fluid density, kg/m^3; η, coefficient of dynamic viscosity, N·sec/m^2; $\nu = \eta/\rho$, coefficient of kinematic viscosity, m^2/sec; F, mass force referred to a mass unit of fluid, N·m^3/kg; p, fluid pressure, N/m^2; λ, coefficient of contact (near-bottom) friction introduced empirically; Re, Reynolds number with allowance for viscous friction; Re$_\lambda$, Reynolds number with allowance for contact friction λ; k, adjustable parameter reflecting the vertical inhomogeneity of the F value with height; h, fluid depth, m; U and D, characteristic values of velocity and length for a given flow, m/sec and m; ψ, horizontal function of current at the upper bound of the fluid layer; V_x and V_y, velocity components in Cartesian coordinates related to the function ψ by the relations $V_x = \partial\psi/\partial y$, $V_y = \partial\psi/\partial x$; $\xi = -\Delta\psi$, vorticity; p_1, parameter of spatial periodicity of the structure of the constant magnetic field; **B**, magnetic induction, T; B_0, amplitude B upon its change in space, T; **H**, H_0, H_z, magnetic field strength, its amplitude and vertical component, A/m; I, electric current, A; j, electric current density, A/m^2; $\mathbf{F}_{MHD}$, mass force of the magnetohydrodynamic nature ($|\mathbf{F}_{MHD}| = F$), N·m^3/kg; x, y, z, Cartesian coordinates; 0 and 0_1, coordinate center and its projection; a, b, m, dimensions of the rectangular cell for generating "mushroom-like structures," m; d_0, thickness of the cell bottom, m; d, c, l, dimensions of the flat rectangular channel, m; δ, width of the insulating liner in the generator of counter jets, m; A_1, A_2, A_3, and A_4, schematical representations of counter colliding and diverging jets; L and L_1, distance between magnets and cell width respectively, m. Subscripts: MHD, magnetohydrodynamic; cr, critical value of a quantity; f, front of the structure of the flow; in, incident flow velocity (on an obstacle); p, permeable spatial structure.

REFERENCES

1. N. F. Bondarenko, M. Z. Gak, and F. V. Dolzhanskii, *Izv. Akad. Nauk SSSR, Fiz. Atmos. Okeana*, **15**, No. 10, 1017–1026 (1979).
2. F. V. Dolzhanskii, V. A. Krymov, and D. Yu. Manin, *Usp. Fiz. Nauk*, **160**, No. 7, 1–47 (1990).

3. F. V. Dolzhansky, V. A. Krymov, and D. Yu. Manin, *Fluid Mech.*, **241**, 705–733 (1992).
4. R. Hide and P. L. Mason, *Adv. Phys.*, **24**, No. 1, 47–60 (1975).
5. A. M. Obukhov, in: *Turbulence and Dynamics of the Atmosphere* [in Russian], Leningrad (1988), pp. 352–366.
6. Yu. L. Chernous'ko, *Izv. Akad. Nauk SSSR, Fiz. Atmos. Okeana*, **16**, No. 4, 423–427 (1980).
7. E. Z. Gak and G. R. Rik, *Dokl. Akad. Nauk SSSR*, **175**, No. 4, 856–858 (1967).
8. E. Z. Gak and G. R. Rik, *Zh. Tekh. Fiz.*, **38**, No. 5, 931–934 (1968).
9. N. F. Bondarenko and M. Z. Gak, *Izv. Akad. Nauk SSSR, Fiz. Atmos. Okeana*, **14**, No. 2, 146–150 (1978).
10. E. Z. Gak, *Inzh.-Fiz. Zh.*, **43**, No. 1, 140–153 (1982).
11. N. F. Bondarenko and E. Z. Gak, *Electromagnetic Phenomena in Natural Waters* [in Russian], Leningrad (1984).
12. N. F. Bondarenko and E. Z. Gak, *Electromagnetic Hydrophysics and Natural Phenomena* [in Russian], Vol. I, St. Petersburg (1994), Vol. II (1995).
13. N. F. Bondarenko, E. Z. Gak, E. E. Rokhinson, and I. P. Anan'ev, *Magnetic Fields in Agricultural Studies and Practice* [in Russian], St. Petersburg (1997).
14. V. A. Krymov, and D. Yu. Manin, *Izv. Ross. Akad. Nauk, Fiz. Atmos. Okeana*, **28**, No. 2, 129–134 (1992).
15. V. A. Dovzhenko and V. A. Krymov, *Izv. Ross. Akad. Nauk, Fiz. Atmos. Okeana*, **27**, No. 8, 879–883 (1991).
16. S. D. Danilov and V. G. Kochina, *Izv. Ross. Akad. Nauk, Fiz. Atmos. Okeana*, **33**, No. 6, 845–849 (1997).
17. S. D. Danilov, F. V. Dolzhanskii, V. A. Dovzhenko, and V. A. Krymov, *Chaos*, **6**, No. 3, 297–306 (1996).
18. N. F. Bondarenko and E. Z. Gak, *Elektron. Obrab. Mater.*, No. 1, 60–63 (1977).
19. V. A. Briksman and V. G. Nevolin, in: *Ext. Abstr. of Papers presented at Xth Riga Meeting on MHD* [in Russian], Vol. 1, Salaspils (1981), pp. 77–78.
20. M. Z. Gak and E. Z. Gak, *Zh. Tekh. Fiz.*, **42**, No. 9, 1992–1994 (1972).
21. N. A. Kudryashev, *Inzh.-Fiz. Zh.*, **72**, No. 6, 1266–1278 (1999).
22. A. G. Alekseev and A. E. Kornev, *Elastic Magnetic Materials* [in Russian], Moscow (1976).
23. S. C. Abrahams and K. Nassaau, in: *Ferroelastic Materials. Encyclopedia of Materials and Engineering*, Oxford (1986), pp. 1690–1692.
24. O. U. V. Fuentes and G. I. F. van Heijst, *Phys. Fluids*, **7**, 2735–2750 (1995).
25. N. Ph. Bondarenko, M. Z. Gak, E. Z. Gak, and M. P. Shapkin, *J. Flow Visualiz. Image Proces.*, **6**, No. 2, 89–94 (1999).
26. A. I. Lazarev, V. V. Kovalenok, and S. V. Avokyan, *Study of the Earth from Piloted Spacecraft* [in Russian], Leningrad (1987).
27. V. I. Gridin and E. Z. Gak, *Physico-Geological Modeling of Natural Phenomena* [in Russian], Moscow (1994).
28. A. N. Kolmogorov, *Dokl. Akad. Nauk SSSR*, **30**, No. 4, 299–303 (1941).
29. V. P. Starr, *Physics of Negative Viscosity Phenomena*, McGraw-Hill, New York–London–San Francisco (1968).
30. G. I. Sivashinsky and V. Yakhot, *Phys. Fluids*, **28**, 1040–1045 (1985).
31. V. Yakhot and G. I. Sivashinsky, *Phys. Rev. A*, **35**, No. 3, 815–820 (1987).
32. E. A. Novikov, in: *Turbulent Flows* [in Russian], Moscow (1974), pp. 85–95.
33. B. J. Cantwell, *Ann. Rev. Fluid Mech.*, **13** , 457–515 (1981).
34. V. V. Zakharchenko, M. N. Kryachko, E. F. Mazhara, V. V. Sevrikov, and N. D. Gavrilenko, *Electrization of Fluids and Its Prevention* [in Russian], Moscow (1975).
35. A. Fage and H. C. H. Townend, *Proc. Roy. Soc. A*, **135** (1932).
36. V. F. Cooper, *Brit. J. Appl. Phys. Suppl.*, No. 2, 11–15 (1953).
37. E. Z. Gak, *Elektron. Obrab. Mater.*, No. 3, 87 (1987); Dep. at VINITI 06.11.1986, No. 7585.
38. M. Z. Gak, *Izv. Akad. Nauk SSSR, Fiz. Atmos. Okeana*, **17**, No. 2, 201–205 (1981).
39. S. D. Danilov and V. A. Dovzhenko, *Izv. Ross. Akad. Nauk, Fiz. Atmos. Okeana*, **31**, No. 5, 621–626 (1995).
40. L. A. Pleshanova, *Izv. Akad. Nauk SSSR, Fiz. Atmos. Okeana*, **18**, No. 4, 339–348 (1982).
41. A. F. Glukhov and G. F. Putin, *Tr. Permsk. Gos. Ped. Inst.*, No. 1, 19–24 (1979).
42. S. O. Belotserkovskii, A. P. Mirabel', and M. A. Chusov, *Izv. Akad. Nauk SSSR, Fiz. Atmos. Okeana*, **14**, No. 1, 11–20 (1978).

43. S. D. Danilov, V. A. Dovzhenko, nd V. G. Kochina, *Izv. Ross. Akad. Nauk, Fiz. Atmos. Okeana*, **32**, No. 6, 777–782 (1996).
44. P. U. Dauxois, S. Fauve, and L. Tuckerman, *Phys. Fluids*, **8**, No. 2, 487–495 (1996).
45. A. Thess, *Phys. Fluids A*, **4**, No. 7, 1385–1407 (1992).
46. N. Platt and L. Sirovich, *Phys. Fluids A*, **3**, No. 4, 681–696 (1991).
47. Y. Nakamura, *Phys. Fluids A*, **9**, No. 11, 3275–3287 (1997).
48. S. Umeda and W. J. Yang, *Int. J. Environ. Pollution*, **10**, No. 2, 289–303 (1996).
49. S. Umeda and W. J. Yang, *Exper. Fluids*, **26**, 389–396 (1999).
50. R. S. Scorer, *Environmental Aerodynamics*, Ellis Horwood Ltd. Press, Div. John Wiley and Sons, New York–London–Sidney–Toronto (1978).
51. F. Sabetta, R. Piva, and M. Di Giacinto, in: *Proc. 14th IUTAM Congr. on Theoretical and Applied Mechanics*, Delft, the Netherlands [Russian translation], Moscow (1979), pp. 656–683.
52. T. Hinz, W. Paul, E. Witte, and A. Munack, in: *Proc. Int. Conf. on Agricultural Engineering*, 20 August–1 September 1994, Milan, Italy (1994), p. 147.
53. N. F. Bondarenko, E. Z. Gak, M. Z. Gak, and É. I. Smolyar, *Dokl. VASKhNIL*, No. 10, 11–13 (1989).
54. E. Z. Gak, E. I. Smolyar, and M. Z. Gak, *Int. Agrophys.*, **6**, No. 1, 59–64 (1994).
55. N. Ph. Bondarenko, E. Z. Gak, M. Z. Gak, and E. I. Smolyar, *Phys. Chem. Earth*, **23**, No. 4, 465–470 (1998).
56. E. Z. Gak and M. Z. Gak, in: *Physics of Soil Water* [in Polish], Warszawa (1996), pp. 31–38.
57. N. F. Bondarenko, E. Z. Gak, and M. P. Shapkin, *Dokl. RASKhN*, No. 1, 45–47 (2002).
58. P. G. Saffman, in: G. K. Batchelor and H. K. Moffatt (eds.), *Modern Hydrodynamics. Advances and Problems* [Russian translation], Moscow (1984), pp. 77–90.
59. V. N. Nikolaevskii, in: *Mechanics. Vortices and Waves* [in Russian], Moscow (1984), pp. 5–7.
60. M. I. Rabinovich and D. I. Trubetskov, in: *Introduction to the Theory of Vibrations and Waves* [in Russian], Moscow–Izhevsk (2000), pp. 448–452.
61. O. M. Belotserkovskii and A. M. Oparin, *Numerical Experiment in Turbulence (From Order to Chaos)* [in Russian], Moscow (2000).